

Video Article

# Preparation of Fungal and Plant Materials for Structural Elucidation Using Dynamic Nuclear Polarization Solid-State NMR

Alex Kirui<sup>1</sup>, Malitha C. Dickwella Widanage<sup>1</sup>, Frederic Mentink-Vigier<sup>2</sup>, Ping Wang<sup>3</sup>, Xue Kang<sup>1</sup>, Tuo Wang<sup>1</sup>

<sup>1</sup>Department of Chemistry, Louisiana State University

<sup>2</sup>National High Magnetic Field Laboratory

<sup>3</sup>Departments of Pediatrics, and Microbiology, Immunology and Parasitology, Louisiana State University Health Sciences Center

\*These authors contributed equally

Correspondence to: Xue Kang at [xkang@lsu.edu](mailto:xkang@lsu.edu), Tuo Wang at [tuowang@lsu.edu](mailto:tuowang@lsu.edu)

URL: <https://www.jove.com/video/59152>

DOI: [doi:10.3791/59152](https://doi.org/10.3791/59152)

Keywords: Solid-state NMR, dynamic nuclear polarization (DNP), carbohydrates, cell walls, biomaterials, plant, fungi

Date Published: 10/31/2018

Citation: Kirui, A., Dickwella Widanage, M.C., Mentink-Vigier, F., Wang, P., Kang, X., Wang, T. Preparation of Fungal and Plant Materials for Structural Elucidation Using Dynamic Nuclear Polarization Solid-State NMR. *J. Vis. Exp.* (), e59152, doi:10.3791/59152 (2018).

## Abstract

This protocol shows how uniformly <sup>13</sup>C, <sup>15</sup>N-labeled fungal materials can be produced and how these soft materials should be proceeded for solid-state NMR and sensitivity-enhanced DNP experiments. The sample processing procedure of plant biomass is also detailed. This method allows the measurement of a series of 1D and 2D <sup>13</sup>C-<sup>13</sup>C/<sup>15</sup>N correlations spectra, which enables high-resolution structural elucidation of complex biomaterials in their native state, with minimal perturbation. The isotope-labeling can be examined by quantifying the intensity in 1D spectra and the polarization transfer efficiency in 2D correlation spectra. The success of dynamic nuclear polarization (DNP) sample preparation can be evaluated by the sensitivity enhancement factor. Further experiments examining the structural aspects of the polysaccharides and proteins will lead to a model of the three-dimensional architecture. These methods can be modified and adapted to investigate a wide range of carbohydrate-rich materials, including the natural cell walls of plants, fungi, algae and bacteria, as well as synthesized or designed carbohydrate polymers and their complex with other molecules.

## Introduction

Carbohydrates play a central role in various biological processes such as energy storage, structural building, and cellular recognition and adhesion. They are enriched in the cell wall, which is a fundamental component in plants, fungi, algae and bacteria<sup>1,2,3</sup>. The cell wall serves as a central source for the production of biofuel and biomaterials, as well as a promising target for antimicrobial therapies<sup>4,5,6,7,8,9</sup>.

The contemporary understanding of these complex materials has been substantially advanced by decades of efforts that were devoted to the structural characterization using four major biochemical or genetic methods. The first major method relies on sequential treatments using harsh chemicals or enzymes to break down the cell walls into different portions, which is followed by compositional and linkage analysis of sugars in each fraction<sup>10</sup>. This method sheds light on the domain distribution of polymers, but the interpretation may be misleading due to the chemical and physical properties of biomolecules. For example, it is difficult to determine whether the alkali-extractable fraction originates from a single domain of less structured molecules or from spatially separated molecules with comparable solubility. Second, the extracted portions or whole cell walls can also be measured using solution NMR to determine the covalent linkages, also termed as crosslinking, between different molecules<sup>11,12,13,14,15</sup>. In this way, the detailed structure of covalent anchors could be probed, but limitations may exist due to the low solubility of polysaccharides, the relatively small number of crosslinking sites, and the ignorance of non-covalent effects that stabilizes polysaccharide packing, including the hydrogen-bonding, van der Waals force, electrostatic interaction and polymer entanglement. Third, the binding affinity has been determined *in vitro* using isolated polysaccharides<sup>16,17,18,19</sup>, but the purification procedures may substantially alter the structure and properties of these biomolecules. This method also fails to replicate the sophisticated deposition and assembly of macromolecules after biosynthesis. Finally, the phenotype, cell morphology and mechanical properties of genetic mutants with attenuated production of certain cell wall component shed lights on the structural functions of polysaccharides, but more molecular evidence is needed to bridge these macroscopic observations with the engineered function of protein machineries<sup>20</sup>.

Recent advances in the development and application of multidimensional solid-state NMR spectroscopy have introduced a unique opportunity for solving these structural puzzles. 2D/3D solid-state NMR experiments enable high-resolution investigation of the composition and architecture of carbohydrate-rich materials in the native state without major perturbation. Structural studies have been successfully conducted on both primary and secondary cell walls of plants, the catalytically treated biomass, bacterial biofilm, the pigment ghosts in fungi and, recently by the authors, the intact cell walls in a pathogenic fungus *Aspergillus fumigatus*<sup>21,22,23,24,25,26,27,28,29,30,31</sup>. The development of dynamic nuclear polarization (DNP)<sup>32,33,34,35,36,37,38,39,40,41,42</sup> substantially facilitates NMR structural elucidation as the sensitivity enhancement by DNP markedly shortens the experimental time on these complex biomaterials. The protocol described here details the procedures for isotope-labeling the fungus *A. fumigatus* and preparing fungal and plant samples for solid-state NMR and DNP characterization. Similar labeling procedures should be applicable to other fungi with altered medium, and the sample preparation procedures should be generally applicable to other carbohydrate-rich biomaterials.

## Protocol

### 1. Growth of $^{13}\text{C}$ , $^{15}\text{N}$ -labeled *Aspergillus fumigatus* Liquid Medium

#### 1. Preparation of unlabeled and $^{13}\text{C}$ , $^{15}\text{N}$ -labeled growth medium

NOTE: Both Yeast Extract Peptone Dextrose medium (YPD) and the improved minimal medium<sup>43</sup> were used for the maintenance of fungal culture. All steps after autoclaving are performed in a laminar flow hood to minimize contamination.

1. Preparation of unlabeled liquid medium: Dissolve 6.5 g of YPD powder in 100 mL of water and then autoclave for 25 min at 134 °C.
2. Preparation of unlabeled solid medium
  1. Add 1.5 g of agar and 6.5 g of YPD powder in 100 mL of distilled water.
  2. Autoclave the medium for 25 min at 121 °C and then cool down to approximately 50 °C.
  3. Transfer 13-15 mL of the medium into each pre-sterile plastic Petri dish and cover the dish using a lid immediately.

#### 3. Preparation of $^{13}\text{C}$ , $^{15}\text{N}$ -labeled liquid medium

NOTE: To prepare the growth solution for isotope labeling, a minimal medium containing  $^{13}\text{C}$ -glucose and  $^{15}\text{N}$ -sodium nitrate and a trace-element solution are prepared separately and then mixed before use.

1. Prepare 100 mL of the isotope-containing minimal medium as listed in **Table 1**. Adjust the pH to 6.6 using NaOH (1 M) or HCl (1M) solution.
2. Autoclave the minimal medium for 25 min at 134 °C.
3. Prepare 100 mL (1000x) of trace elements solution, dissolve the salts listed in **Table 2** in the distilled water. Autoclave the solution for 25 min at 134 °C. Cool down and store the solution at 4 °C for short-term use. The pH will be about 6.5 and can be checked using a pH meter.
4. Add 0.1 mL of trace elements solution to 100 mL of  $^{13}\text{C}$ ,  $^{15}\text{N}$ -labeled minimal medium as listed in **Table 2** before use.

#### 2. Growth of the fungal materials

1. Transfer a small amount of fungi from the storage onto a YPD plate using an inoculating loop in a laminar flow hood. Keep the culture at 30 °C for 2 days in an incubator.
2. Use an inoculating loop to transfer an active growing fungal edge to the  $^{13}\text{C}$ ,  $^{15}\text{N}$ -labeling solution in a laminar flow hood. Keep the culture at 30 °C for 3-5 days at 220 rpm in a shaking incubator.
3. Centrifuge at 4000 x g for 20 min. Remove the supernatant and collect the pellet.
4. Use a tweezer to collect ~0.5 g of well-hydrated pellet (>50 wt% hydration) for NMR studies. Loss of hydration at any point will substantially worsen the spectral resolution.  
NOTE: If needed, a small amount (0.1 g) of the hydrated mycelia can be separated and fully dried under  $\text{N}_2$  gas flow in a hood or a lyophilizer to estimate the hydration level and calculate the dry mass percentage. Usually, a pellet containing ~0.3 g dry mass can be obtained after 3 days. If the NMR experiment to be conducted is long (>7 days) and/or if the state of the fungi needs to be fixed, the fungal material can be deeply frozen in liquid  $\text{N}_2$  for 10-20 min before further processing. If the experiment will be short (3-6 days), the freezing can be skipped so that the sample can remain fresh.
5. Mix the excess material with 20% (v/v) of glycerol in a centrifuge tube and keep it in a -80 °C freezer for long-term storage.

### 2. Preparation of *A. fumigatus* for Solid-state NMR and DNP Studies

#### 1. Preparation of *A. fumigatus* for solid-state NMR experiments

1. Dialyze the  $^{13}\text{C}$ ,  $^{15}\text{N}$ -labeled fungal sample (Step 1.2.4.) against 1 L of 10 mM phosphate buffer (pH 7.0) at 4 °C using a dialysis bag with a 3.5 kDa molecular weight cutoff to remove small molecules from the growth medium for a total period of 3 days. Change the buffer twice daily.  
NOTE: Alternatively, the sample could be washed for 6-10 times using deionized water to remove residual small molecules.
2. Transfer the sample into a 15 mL tube and centrifuge for 5 min (10,000 x g) using a benchtop centrifuge. Remove the supernatant and collect the remaining fungal materials.
3. Pack 70-80 mg of the uniformly  $^{13}\text{C}$ -labeled and well-hydrated sample paste into a 4-mm  $\text{ZrO}_2$  rotor or 30-50 mg to 3.2 mm rotors for NMR experiments. Repetively squeeze the sample gently using a metal rod and absorb the excess water using paper.
4. Tightly cap the rotor and insert the sample into the spectrometer for solid-state NMR characterization.  
NOTE: The brand-new rotors are suggested to minimize the possibility of rotor crash and sample spill in the NMR spectrometer. If needed, a disposable Kel-F insert with sealing screws can be used to serve as a secondary container inside the rotor.

#### 2. Preparation of *A. fumigatus* samples for DNP experiments

1. Prepare 100  $\mu\text{L}$  of DNP solvents<sup>29,44</sup> (also known as the DNP matrix) in a 1.5 mL microcentrifuge tube for  $^{13}\text{C}$ ,  $^{15}\text{N}$ -labeled fungal samples. This DNP matrix contains a mixture of  $\text{d}_8$ -glycerol/ $\text{D}_2\text{O}$ / $\text{H}_2\text{O}$  (60/30/10 Vol%).  
NOTE: If unlabeled samples are to be investigated, then prepare the DNP matrix using  $^{13}\text{C}$ -depleted  $\text{d}_8$ -glycerol ( $^{12}\text{C}_3$ , 99.95%;  $\text{D}_8$ , 98%) and  $\text{D}_2\text{O}$  and  $\text{H}_2\text{O}$  to avoid  $^{13}\text{C}$  signal contribution from the solvents.
2. Dissolve 0.7 mg of AMUPol<sup>45</sup> in 100  $\mu\text{L}$  of DNP solvents to form 10 mM radical stock solution. Vortex for 2-3 min to ensure that radicals are fully dissolved in the solution.
3. Soak 10 mg of the dialyzed  $^{13}\text{C}$ ,  $^{15}\text{N}$ -labeled fungal materials as described in prior steps (Steps 2.1.1 and 2.1.2) into 50  $\mu\text{L}$  of AMUPol solution, and mildly grind the mixture using a pestle and a mortar to ensure penetration of the radicals into the porous cell walls.  
NOTE: To reduce the rate of hydration loss, the grinding can also take place in a microcentrifuge tube using a micropestle.
4. Add another 30  $\mu\text{L}$  of the radical solution to the grinded pellet to further hydrate the fungal sample.

5. Pack the pellet into a 3.2-mm sapphire rotor, squeeze mildly and remove the excess DNP solvent. Add a 3.2-mm silicone plug to prevent the loss of hydration. Typically, 5-30 mg of sample can be packed to the rotor. The exact amount needs to be determined by the sensitivity requirement of the NMR experiments to be conducted.
6. Insert and spin up the sample in a DNP spectrometer, measure a DNP-enhanced spectrum under microwave irradiation and compare it with the microwave-off spectrum. This will lead to an enhancement factor  $\epsilon_{\text{on/off}}$ , which should be 20-40 for these complex materials. Run the designed experiments to determine cell wall structure.

### 3. Preparation of Plant Biomass for NMR and DNP Studies

1. Preparation of plant materials for solid-state NMR
  1. Produce uniformly  $^{13}\text{C}$ -labeled plants in-house using  $^{13}\text{CO}_2$  supplies in a growth chamber or  $^{13}\text{C}$ -glucose medium as described previously<sup>46,47</sup> or directly purchase labeled materials from isotope-labeling companies.  
NOTE:  $^{13}\text{C}$ -glucose can only be used in dark growth to avoid the introduction of  $^{12}\text{C}$  by photosynthesis.
  2. Cut the uniformly  $^{13}\text{C}$  labeled plant material into small pieces (typically 1-2 mm in dimension) using a laboratory razor blade.  
NOTE: Depending on the purpose, the extracted cell walls are sometimes used for structural characterization and the detailed protocols are reported in previous studies<sup>21,46</sup>.
  3. If the sample was previously dried, add 100  $\mu\text{L}$  of water to 30 mg of plant materials in a 1.5 mL microcentrifuge tube, vortex, equilibrate at room temperature for 1 day. Centrifuge at 4000 x g for 10 min and remove the excess water using a pipette.
  4. If the sample was never-dried at any point, directly use the sample without further treatment.
  5. Pack the resulting plant materials into 3.2-mm or 4-mm  $\text{ZrO}_2$  rotors for solid-state NMR experiments.
2. Preparation of plant materials for DNP studies
  1. Prepare 60  $\mu\text{L}$  stock solution of 10 mM AMUPol radical as described steps 2.2.1 and 2.2.2.
  2. Cut the uniformly  $^{13}\text{C}$  labeled plant material to be studied into small pieces (1-2 mm in dimension) using a laboratory razor blade and weigh 20 mg of the plant materials.
  3. Hand-grind the plant pieces into small particles (~1-2 mm in size) using a mortar and pestle. The final powders have a homogenous appearance.
  4. Add 40  $\mu\text{L}$  of the DNP stock solution prepared in prior step (Step 2.2.2) to the plant material and grind mildly for 5 min to ensure homogeneous mixing with the radical.
  5. Add another 20  $\mu\text{L}$  of the stock solution to further hydrate the plant material after grinding.
  6. Pack the equilibrated plant sample into a 3.2-mm sapphire rotor for DNP experiments. Insert a silicone plug to avoid the loss of hydration.

### 4. Standard Solid-State NMR Experiments for Initial Characterization of Carbohydrate-Rich Biomaterials

NOTE: A brief overview of the NMR experiments is provided in this section. However, structural elucidation typically requires extensive expertise. Therefore, collaborative efforts with NMR spectroscopists is recommended.

1. Measure 1D  $^{13}\text{C}$  Cross Polarization (CP),  $^{13}\text{C}$  Direct Polarization (DP) with 2-s and 35-s recycle delays, and  $^1\text{H}$ - $^{13}\text{C}$  INEPT<sup>48,49</sup> spectra to obtain a general understanding of the dynamical distribution of cell components (**Figure 1a**). The cell walls are typically the relatively rigid portion and exhibit dominant signals in the CP spectrum.
2. Measure a series of standard 2D  $^{13}\text{C}$ - $^{13}\text{C}$  correlation experiments for resonance assignments of  $^{13}\text{C}$  signals. Start with refocused INADEQUATE<sup>50,51</sup> to obtain carbon connectivity, which need to be assisted by a series of through-space experiments such as 1.5-ms RFDR<sup>52</sup> (**Figure 1b**) and 50-ms CORD/DARR<sup>53</sup> experiments.  
NOTE: If it is of interest to find a sample rich in a specific component, for example, the primary or secondary cell walls, then multiple segments or multiple plants may need to be measured separately to find the sample with the optimal composition.
3. Conduct 2D  $^{15}\text{N}$ - $^{13}\text{C}$  correlation experiments which can be measured to facilitate the resonance assignments of proteins and nitrogenated carbohydrates.  
NOTE: The resonance assignment is typically time-consuming. A method is currently being developed to facilitate the resonance assignment of carbohydrate signals for those scientists without prior experience.
4. Measure more specialized experiments to determine the spatial proximities (**Figure 1c, d**), hydration and mobilities of complex biomolecules to determine the three-dimensional structure of the carbohydrate-rich materials as systematically described previously<sup>22,29</sup>.

### Representative Results

The isotope labeling substantially enhances the NMR sensitivity and makes it possible for measuring a series of 2D  $^{13}\text{C}$ - $^{13}\text{C}$  and  $^{13}\text{C}$ - $^{15}\text{N}$  correlation spectra to analyze the composition, hydration, mobility and packing of polymers, which will be integrated to construct a three-dimensional model of cell wall architecture (**Figure 1**). If the uniform labeling succeeds, a complete set of 1D  $^{13}\text{C}$  and  $^{15}\text{N}$  spectra can be collected within 1 h and each standard 2D spectrum should take no longer than 24 h of measurement.

Well-prepared samples usually expect both high NMR intensities and sharp lines. Compromising of either parameter indicates un-optimized sample preparation. The fungal samples should be prepared in a never-dried manner, and partial dehydration during the packing steps could lead to a notable broadening of the linewidth. If the experimental time is substantially longer than expected for a fully packed NMR sample, the labeling level might be low. If off-diagonal signals are difficult to obtain in the 2D  $^{13}\text{C}$ - $^{13}\text{C}$  correlation spectrum, statistical labeling might have occurred (**Figure 1b**). The two  $^{13}\text{C}$  peaks at 96 and 92 ppm are signature carbon 1 signals of glucose<sup>54</sup>, therefore, their strong intensities in the quantitative  $^{13}\text{C}$  direct polarization (DP) spectra measured with long recycle delays of 35 s typically indicate the dominance of small molecules due to incomplete dialysis or washing (**Figure 1a**). With well-labeled samples, long-range correlations can be further measured to detect the spatial proximities of biomolecules (**Figure 1c**) and construct the structural model of intact cell walls (**Figure 1d**).

Chemical name	Chemical formula	Concentration (gram per liter)
Dipotassium Phosphate	$\text{K}_2\text{HPO}_4$	1.045 g
Magnesium Sulfate Heptahydrate	$\text{MgSO}_4 \cdot 7\text{H}_2\text{O}$	0.52 g
Monopotassium Phosphate	$\text{KH}_2\text{PO}_4$	0.815 g
$^{15}\text{N}$ - Sodium Nitrate	$^{15}\text{NaNO}_3$	6.0 g
Potassium Chloride	KCl	0.52 g
U- $^{13}\text{C}$ -Glucose	$^{13}\text{C}_6\text{H}_{12}\text{O}_6$	10.0 g

**Table 1. The composition of the minimal medium.**

Chemical name	Chemical formula	Concentration (g/L)
Ammonium Molybdate Tetrahydrate	$(\text{NH}_4)_6\text{Mo}_7\text{O}_{24} \cdot 4\text{H}_2\text{O}$	11 g
Boric acid	$\text{H}_3\text{BO}_3$	11 g
Cobaltous Chloride Hexahydrate	$\text{CoCl}_2 \cdot 6\text{H}_2\text{O}$	16 g
Cupric Sulfate Pentahydrate	$\text{CuSO}_4 \cdot 5\text{H}_2\text{O}$	16 g
Ferrous Sulfate Heptahydrate	$\text{FeSO}_4 \cdot 7\text{H}_2\text{O}$	5 g
Manganous Chloride Tetrahydrate	$\text{MnCl}_2 \cdot 4\text{H}_2\text{O}$	5 g
Tetrasodium Ethylenediaminetetraacetate	$\text{Na}_4\text{EDTA} \cdot 4\text{H}_2\text{O}$	60 g
Zinc Sulfate Heptahydrate	$\text{ZnSO}_4 \cdot 7\text{H}_2\text{O}$	22 g

**Table 2. The composition of the trace-element solution (concentrated).** Note that for preparing unlabeled fungi, unlabeled glucose and unlabeled sodium nitrate can be used.

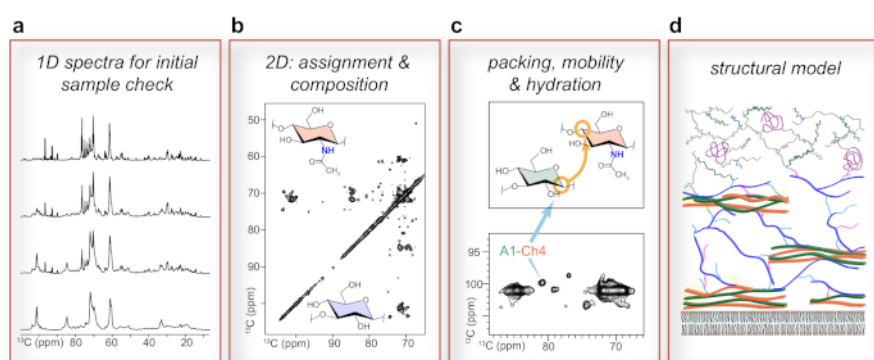


**Figure 1. Flowchart for characterizing fungal cell wall structure using solid-state NMR.** (a) 1D spectra for initial sample screening. From the top to the bottom are INEPT,  $^{13}\text{C}$  DP with 2-s recycle delays,  $^{13}\text{C}$  DP with 35-s recycle delays and  $^{13}\text{C}$  CP spectra, with decreasing mobility for the detected molecules. (b) 2D  $^{13}\text{C}$ - $^{13}\text{C}$  correlation spectrum measured using 1.5-ms RFDR recoupling. (c) Representative intermolecular cross peak detected using 15-ms PAR spectrum. (d) Structural model obtained from NMR data. Panels a, c and d have been modified from Kang *et al.*, *Nat. Commun.* 9, 2747 (2018). [Please click here to view a larger version of this figure.](#)

## Discussion

Compared with the biochemical methods, solid-state NMR has advantages as a non-destructive and high-resolution technique. NMR is also quantitative in compositional analysis, and unlike most other analytical methods, does not have the uncertainties introduced by the limited solubility of biopolymers. Establishment of the current protocol facilitates future studies on carbohydrate-rich biomaterials and functionalized polymers. However, it should be noted that the resonance assignment and data analysis can be time-consuming and usually require systematic training. The authors are currently developing tools and databases to help scientists without prior experience to overcome this barrier.

Since the natural isotope abundance of  $^{13}\text{C}$  is only 1.1%, the probability for observing a  $^{13}\text{C}$ - $^{13}\text{C}$  cross peak using unlabeled materials is only 0.012% (1.1% x 1.1%) of that using uniformly labeled samples. Therefore, the isotope enrichment achieved using this protocol substantially enhances the NMR sensitivity by four orders of magnitude and enables 2D correlation experiments for structural determination.

The optimized, well-hydrated samples should exhibit sharp lines in 2D  $^{13}\text{C}$ - $^{13}\text{C}$  correlation spectra. The mobile components, such as the  $\beta$ -glucans in *A. fumigatus* and the pectins in plants should exhibit a full-width at half-maximum (FWHM) linewidth of 0.3-0.5 ppm on 600-800 MHz NMR spectrometers<sup>29,31</sup>. The rigid components have slightly broader peaks due to conformational heterogeneity of the constituting, repetitive sugar units and the lack of rapid molecular motions. The typical  $^{13}\text{C}$  linewidth is 0.7-1.0 ppm for cellulose microfibrils in plants and 0.5-0.7 ppm for chitin in fungi<sup>55</sup>. The sharp linewidth of cellulose and chitin are mainly caused by polymer crystallinity, thus is partially resistant to dehydration and temperature change, for example, the cryogenic temperature of DNP experiment<sup>56,57</sup>. The peak sharpness of matrix polymers, however, are highly sensitive to the change of sample conditions that affect the polymer mobility, therefore, it can be used as an indicator of sample hydration. Broad lines of matrix polymers typically designate the lack of hydration in the sample, which may be fully or partially recovered by re-adding water<sup>58</sup>. Typically, a hydration level of 50-80 wt% is enough for providing a good linewidth in both plant and fungal samples.

DNP is often necessary for investigating these challenging whole-cell systems. Typically, a 20-40 fold enhancement of sensitivity could be achieved on an optimized sample on a 600 MHz/395 GHz DNP spectrometer and this value increases with decreasing field, for example, almost doubled on a 400 MHz/263 GHz DNP<sup>26,59</sup>. There are several factors that could affect the DNP efficiency. First, the penetration of radicals into the porous network of cell walls is crucial and this process can be substantially facilitated by mild grinding of the biomaterials in the radical-containing DNP matrix. Second, the physical properties, the stiffness for example, of the sample affects the choice of microwave power, the DNP matrix "melts" under 12 W irradiation as evidenced by the sharpening of  $^1\text{H}$  resonances, which was not a problem for the stiffer plant stems. As a result, a more isotropic pattern of the  $^1\text{H}$  solvent peak is observed, with substantially lower spinning sidebands and attenuated DNP enhancement. Therefore, weaker power is recommended for softer materials. Third, the composition of DNP matrix should be optimized. It turns out that  $\text{d}_8$ -glycerol/ $\text{D}_2\text{O}/\text{H}_2\text{O}$  is generally the best solvents for soft materials while a simpler and cheaper choice of  $\text{D}_2\text{O}/\text{H}_2\text{O}$  can also be effective in some cases because the sugars present in the system serves as cryoprotectants to some extent. In contrast, the  $\text{d}_6$ -DMSO/ $\text{D}_2\text{O}/\text{H}_2\text{O}$  solution fails in both plants and fungal samples, with less than 10-fold of sensitivity enhancement, thus it is not recommended for use unless for special purposes. A matrix-free protocol has recently been demonstrated to be highly effective due to solvent depletion, which creates additional space to accommodate more materials<sup>34,56,60</sup>. However, the loss of hydration presents a major perturbation to the structure of biomolecules, thus this method might not be suitable for biological systems. If unlabeled cell walls are to be studied,  $^{13}\text{C}$ -depleted  $\text{d}_8$ -glycerol/ $\text{D}_2\text{O}/\text{H}_2\text{O}$  is the optimal solvent that does not contribute any natural abundance  $^{13}\text{C}$  signals nor sacrifices any sensitivity enhancement.

## Disclosures

We have nothing to disclose.

## Acknowledgements

This work was supported by National Science Foundation through NSF OIA-1833040. The National High Magnetic Field Laboratory (NHMFL) is supported by National Science Foundation through DMR-1157490 and the State of Florida. The MAS-DNP system at NHMFL is funded in part by NIH S10 OD018519 and NSF CHE-1229170.

## References

- Murrey, H. E., & Hsieh-Wilson, L. C. The chemical neurobiology of carbohydrates. *Chemical Reviews*. **108** (5), 1708-1731, (2008).
- Latge, J. P. The cell wall: a carbohydrate armour for the fungal cell. *Molecular Microbiology*. **66** (2), 279-290, (2007).
- Cosgrove, D. J. Growth of the plant cell wall. *Nature Reviews Molecular Cell Biology*. **6** (11), 850-861, (2005).
- Furtado, A. *et al.* Modifying plants for biofuel and biomaterial production. *Plant Biotechnology Journal*. **12** (9), 1246-1258, (2014).
- Loqué, D., Scheller, H. V., & Pauly, M. Engineering of plant cell walls for enhanced biofuel production. *Current Opinion in Plant Biology*. **25**, 151-161, (2015).
- Latge, J. P. *Aspergillus fumigatus* and aspergillosis. *Clinical Microbiology Reviews*. **12** (2), 310-350, (1999).
- Ragauskas, A. J. *et al.* The path forward for biofuels and biomaterials. *Science*. **311** (5760), 484-489, (2006).
- Service, R. F. Cellulosic ethanol - Biofuel researchers prepare to reap a new harvest. *Science*. **315** (5818), 1488-1491, (2007).
- Somerville, C., Youngs, H., Taylor, C., Davis, S. C., & Long, S. P. Feedstocks for Lignocellulosic Biofuels. *Science*. **329** (5993), 790-792, (2010).
- Schiavone, M. *et al.* A combined chemical and enzymatic method to determine quantitatively the polysaccharide components in the cell wall of yeasts. *FEMS Yeast Research*. **14** (6), 933-947, (2014).
- Cheng, K., Sorek, H., Zimmermann, H., Wemmer, D. E., & Pauly, M. Solution-State 2D NMR Spectroscopy of Plant Cell Walls Enabled by a Dimethylsulfoxide- $\text{d}(6)/1$ -Ethyl-3-methylimidazolium Acetate Solvent. *Analytical Chemistry*. **85** (6), 3213-3221, (2013).
- Mansfield, S. D., Kim, H., Lu, F. C., & Ralph, J. Whole plant cell wall characterization using solution-state 2D NMR. *Nature Protocols*. **7** (9), 1579-1589, (2012).
- Tan, L. *et al.* An Arabidopsis Cell Wall Proteoglycan Consists of Pectin and Arabinoxylan Covalently Linked to an Arabinogalactan Protein. *Plant Cell*. **25** (1), 270-287, (2013).
- Kollar, R., Petrakova, E., Ashwell, G., Robbins, P. W., & Cabib, E. Architecture of the Yeast-Cell Wall - the Linkage between Chitin and Beta(1-3)-Glucan. *Journal of Biological Chemistry*. **270** (3), 1170-1178, (1995).
- Kollar, R. *et al.* Architecture of the yeast cell wall - beta(1->6)-glucan interconnects mannoprotein, beta(1-3)-glucan, and chitin. *Journal of Biological Chemistry*. **272** (28), 17762-17775, (1997).
- Mccann, M. C. *et al.* Old and new ways to probe plant cell wall architecture. *Canadian Journal of Botany*. **73** S103-S113, (1995).



17. Whitney, S. E. C., Brigham, J. E., Darke, A. H., Reid, J. S. G., & Gidley, M. J. In-Vitro Assembly of Cellulose/Xyloglucan Networks - Ultrastructural and Molecular Aspects. *The Plant Journal*. **8** (4), 491-504, (1995).
18. Zykwska, A. W., Ralet, M. C. J., Garnier, C. D., & Thibault, J. F. J. Evidence for *in vitro* binding of pectin side chains to cellulose. *Plant Physiology*. **139** (1), 397-407, (2005).
19. Kiemle, S. N. *et al.* Role of (1,3)(1,4)-beta-Glucan in Cell Walls: Interaction with Cellulose. *Biomacromolecules*. **15** (5), 1727-1736, (2014).
20. Pogorelko, G., Lionetti, V., Bellincampi, D., & Zabolina, O. Cell wall integrity: targeted post-synthetic modifications to reveal its role in plant growth and defense against pathogens. *Plant Signaling & Behavior*. **8** (9), e25435, (2013).
21. Wang, T., Park, Y. B., Cosgrove, D. J., & Hong, M. Cellulose-Pectin Spatial Contacts Are Inherent to Never-Dried *Arabidopsis thaliana* Primary Cell Walls: Evidence from Solid-State NMR. *Plant Physiology*. **168** (3), 871-884, (2015).
22. Wang, T., Salazar, A., Zabolina, O. A., & Hong, M. Structure and dynamics of *Brachypodium* primary cell wall polysaccharides from two-dimensional <sup>13</sup>C solid-state nuclear magnetic resonance spectroscopy. *Biochemistry*. **53** (17), 2840-2854, (2014).
23. Grantham, N. J. *et al.* An even pattern of xylan substitution is critical for interaction with cellulose in plant cell walls. *Nature Plants*. **3** (11), 859-865, (2017).
24. Simmons, T. J. *et al.* Folding of xylan onto cellulose fibrils in plant cell walls revealed by solid-state NMR. *Nature Communications*. **7** 13902, (2016).
25. Komatsu, T., & Kikuchi, J. Selective Signal Detection in Solid-State NMR Using Rotor-Synchronized Dipolar Dephasing for the Analysis of Hemicellulose in Lignocellulosic Biomass. *The Journal of Physical Chemistry Letters*. **4** (14), 2279-2283, (2013).
26. Perras, F. A. *et al.* Atomic-Level Structure Characterization of Biomass Pre- and Post-Lignin Treatment by Dynamic Nuclear Polarization-Enhanced Solid-State NMR. *The Journal of Physical Chemistry A*. **121** (3), 623-630, (2017).
27. Chatterjee, S., Prados-Rosales, R., Itin, B., Casadevall, A., & Stark, R. E. Solid-state NMR Reveals the Carbon-based Molecular Architecture of *Cryptococcus neoformans* Fungal Eumelanins in the Cell Wall. *Journal of Biological Chemistry*. **290** (22), 13779-13790, (2015).
28. Zhong, J., Frases, S., Wang, H., Casadevall, A., & Stark, R. E. Following fungal melanin biosynthesis with solid-state NMR: biopolymer molecular structures and possible connections to cell-wall polysaccharides. *Biochemistry*. **47** (16), 4701-4710, (2008).
29. Kang, X. *et al.* Molecular architecture of fungal cell walls revealed by solid-state NMR. *Nature Communications*. **9** (1), 2747, (2018).
30. Takahashi, H. *et al.* Solid-state NMR on bacterial cells: selective cell wall signal enhancement and resolution improvement using dynamic nuclear polarization. *Journal of the American Chemical Society*. **135** (13), 5105-5110, (2013).
31. Wang, T., & Hong, M. Solid-state NMR investigations of cellulose structure and interactions with matrix polysaccharides in plant primary cell walls. *Journal of Experimental Botany*. **67** 503-514, (2016).
32. Mentink-Vigier, F., Akbey, Ü., Oschkinat, H., Vega, S., & Feintuch, A. Theoretical aspects of magic angle spinning-dynamic nuclear polarization. *Journal of Magnetic Resonance*. **258** 102-120, (2015).
33. Gupta, R. *et al.* Dynamic nuclear polarization enhanced MAS NMR spectroscopy for structural analysis of HIV-1 protein assemblies. *The Journal of Physical Chemistry B*. **120** (2), 329-339, (2016).
34. Takahashi, H., Hediger, S., & De Paëpe, G. Matrix-free dynamic nuclear polarization enables solid-state NMR <sup>13</sup>C-<sup>13</sup>C correlation spectroscopy of proteins at natural isotopic abundance. *Chemical Communications*. **49** (82), 9479-9481, (2013).
35. Ni, Q. Z. *et al.* High frequency dynamic nuclear polarization. *Accounts of Chemical Research*. **46** (9), 1933-1941, (2013).
36. Koers, E. J. *et al.* NMR-based structural biology enhanced by dynamic nuclear polarization at high magnetic field. *Journal of Biomolecular NMR*. **60** (2-3), 157-168, (2014).
37. Saliba, E. P. *et al.* Electron Decoupling with Dynamic Nuclear Polarization in Rotating Solids. *Journal of the American Chemical Society*. **139** (18), 6310-6313, (2017).
38. Mentink-Vigier, F. *et al.* Efficient cross-effect dynamic nuclear polarization without depolarization in high-resolution MAS NMR. *Chemical Science*. **8** (12), 8150-8163, (2017).
39. Smith, A. N., Twahir, U. T., Dubroca, T., Fanucci, G. E., & Long, J. R. Molecular Rationale for Improved Dynamic Nuclear Polarization of Biomembranes. *The Journal of Physical Chemistry B*. **120** (32), 7880-7888, (2016).
40. Su, Y., Andreas, L., & Griffin, R. G. Magic angle spinning NMR of proteins: high-frequency dynamic nuclear polarization and <sup>1</sup>H detection. *Annual Reviews of Biochemistry*. **84** 465-497, (2015).
41. Hediger, S., Lee, S., Mentink-Vigier, F., & Paëpe, G. D. MAS-DNP Enhancements : Hyperpolarization , Depolarization , and Absolute Sensitivity. *eMagRes*. **7** 1-13, (2018).
42. Ni, Q. Z. *et al.* In Situ Characterization of Pharmaceutical Formulations by Dynamic Nuclear Polarization Enhanced MAS NMR. *The Journal of Physical Chemistry B*. **121** (34), 8132-8141, (2017).
43. Hill, T. W., & Kafer, E. Improved protocols for *Aspergillus* minimal medium: trace element and minimal medium salt stock solutions. *Fungal Genetics Reports*. **48** (1), 20-21, (2001).
44. Rossini, A. J. *et al.* Dynamic nuclear polarization surface enhanced NMR spectroscopy. *Accounts of Chemical Research*. **46** (9), 1942-1951, (2013).
45. Sauvée, C. *et al.* Highly efficient, water-soluble polarizing agents for dynamic nuclear polarization at high frequency. *Angewandte Chemie International Edition*. **125** (41), 11058-11061, (2013).
46. Phyto, P. *et al.* Gradients in Wall Mechanics and Polysaccharides along Growing Inflorescence Stems. *Plant physiology*. **175** (4), 1593-1607, (2017).
47. White, P. B., Wang, T., Park, Y. B., Cosgrove, D. J., & Hong, M. Water-polysaccharide interactions in the primary cell wall of *Arabidopsis thaliana* from polarization transfer solid-state NMR. *Journal of the American Chemical Society*. **136** (29), 10399-10409, (2014).
48. Jippo, T., Kamo, O., & Nagayama, K. Determination of long-range proton-carbon <sup>13</sup>C coupling constants with selective two-dimensional INEPT. *Journal of Magnetic Resonance* (1969). **66** (2), 344-348, (1986).
49. Morris, G. A. Sensitivity enhancement in nitrogen-15 NMR: polarization transfer using the INEPT pulse sequence. *Journal of the American Chemical Society*. **102** (1), 428-429, (1980).
50. Cadars, S. *et al.* The refocused INADEQUATE MAS NMR experiment in multiple spin-systems: interpreting observed correlation peaks and optimising lineshapes. *Journal of Magnetic Resonance*. **188** (1), 24-34, (2007).
51. Lesage, A., Bardet, M., & Emsley, L. Through-bond carbon-carbon connectivities in disordered solids by NMR. *Journal of the American Chemical Society*. **121** (47), 10987-10993, (1999).
52. Bennett, A. E. *et al.* Homonuclear radio frequency-driven recoupling in rotating solids. *The Journal of Chemical Physics*. **108** (22), 9463-9479, (1998).

53. Lu, X., Guo, C., Hou, G., & Polenova, T. Combined zero-quantum and spin-diffusion mixing for efficient homonuclear correlation spectroscopy under fast MAS: broadband recoupling and detection of long-range correlations. *Journal of Biomolecular NMR*. **61** (1), 7-20, (2015).
54. Wang, T., Zabolina, O., & Hong, M. Pectin-cellulose interactions in the Arabidopsis primary cell wall from two-dimensional magic-angle-spinning solid-state nuclear magnetic resonance. *Biochemistry*. **51** (49), 9846-9856, (2012).
55. Wang, T., Yang, H., Kubicki, J. D., & Hong, M. Cellulose Structural Polymorphism in Plant Primary Cell Walls Investigated by High-Field 2D Solid-State NMR Spectroscopy and Density Functional Theory Calculations. *Biomacromolecules*. **17** (6), 2210-2222, (2016).
56. Kirui, A. *et al.* Atomic Resolution of Cotton Cellulose Structure Enabled by Dynamic Nuclear Polarization Solid-State NMR. *Cellulose*. accepted, (2019).
57. Wang, T. *et al.* Sensitivity-enhanced solid-state NMR detection of expansin's target in plant cell walls. *Proceedings of the National Academy of Sciences of the United States of America*. **110** (41), 16444-16449, (2013).
58. Wang, T., Park, Y. B., Cosgrove, D. J., & Hong, M. Cellulose-Pectin Spatial Contacts Are Inherent to Never-Dried Arabidopsis thaliana Primary Cell Walls: Evidence from Solid-State NMR. *Plant Physiology*. **168** (3), 871-884, (2015).
59. Liao, S. Y., Lee, M., Wang, T., Sergeyev, I. V., & Hong, M. Efficient DNP NMR of membrane proteins: sample preparation protocols, sensitivity, and radical location. *Journal of Biomolecular NMR*. **64** (3), 223-237, (2016).
60. Takahashi, H. *et al.* Rapid Natural-Abundance 2D <sup>13</sup>C-<sup>13</sup>C Correlation Spectroscopy Using Dynamic Nuclear Polarization Enhanced Solid-State NMR and Matrix-Free Sample Preparation. *Angewandte Chemie International Edition*. **51** (47), 11766-11769, (2012).